JOURNAL OF MATERIALS SCIENCE 20 (1985) 1985–1992

# Relationship between fracture topography and fracture toughness of a high strength steel

M. O. LAI, W. G. FERGUSON*
*Mechanical Engineering Department, National University of Singapore, Kent Ridge, Singapore*

The relationship between fracture topography and the plane strain fracture toughness of Comsteel En25 tempered at nine different temperatures and with crack planes in the R–L, R–C and L–R orientations has been studied. The results show that fracture toughness is qualitatively relatable to the fracture morphology. Due to the shape and alignment of the elongated MnS inclusions, fracture toughness in the L–R orientation was found to be 1.8 times those in the other two orientations. Terrace-type fracture prevailed in the R–L orientation, but this frequently was observed to change to zigzag type fracture in the R–C orientation. However, both these fracture mechanisms were absent in the L–R orientation.

## 1. Introduction

Tempering decreases the brittleness of martensite but increases its ductility. Like other material properties, tempering has a great influence on the plane strain fracture toughness as well. Due to the change in ductility, fracture mechanisms will be altered. However, unlike the dependence of yield stress on tempering which is better understood, the tempering effect on fracture toughness has not heretofore been predictable. In addition, non-metallic inclusions can have a very dramatic effect on the properties and behaviour of steel. It has been shown that in general inclusions have a detrimental effect on fracture toughness [1–4]. The effect is partly due to fibering commonly found in rolled products, and partly to chemical-segregation banding in the material [5]. As a result, it is easier for a crack to propagate in a direction parallel to the alignment of the inclusions. The effects of tempering and anistropy are reflected in the fracture topography of the test specimens. Hence, fractographic characterization has been found to be extremely valuable in determining the influence of these factors on other properties. The present investigation studies qualitatively the relationship between fracture topography and plane strain fracture toughness of Comsteel En25, tempered at various temperatures and fractured with the crack plane in the R–L, R–C and L–R orientations.

## 2. Experimental procedure

### 2.1. Material

The specimen material used in the investigation was Comsteel En25, a high-strength low-alloy steel supplied in the form of 125 mm diameter black bar; in the as-received condition it was heat treated and hardened to 950–1100 MPa tensile strength. A typical chemical composition was 0.31% carbon, 0.26% silicon, 0.58% manganese 2.22% nickel, 0.59% chromium, 0.53% molybdenum, 0.025% phosphorus and 0.032% sulphur.

### 2.2. Specimen preparation and testing

25 mm thick compact tension specimens of dimensions in accordance with the ASTM standard E399–81 specification were machined from the bar so that the crack plane was in the R–L or C–L

*Present address:* Chemical and Materials Engineering Department, University of Auckland, New Zealand.

0022–2461/85 $03.00 + .12 © *1985 Chapman and Hall Ltd.* 

orientation. All specimens were austenitized at 850° C in a salt bath for an hour and then quenched into a flowing column of oil. Apart from the as-quenched specimens, all other specimens were tempered for one hour at each of the following temperatures: 100, 200, 300, 400, 450, 500, 550 and 600° C. In many cases, three specimens were tested at each tempering temperature. In order to study the effect of anisotropy on fracture topography, compact tension specimens with crack planes in the R–C and L–R orientations were likewise machined. However, only a tempering temperature of 500° C was chosen in these investigations.

Specimens were fatigue precracked and fracture tested with an MTS electrohydraulic machine using the procedure set out in the ASTM standard. During the fracture test, the displacements were measured using a standard double-cantilever beam clip gauge fixed on to the specimen by means of attachable knife-edges. Load and displacement outputs were recorded on an X–Y recorder.

The fracture surfaces of the specimens were washed with acetone in an ultrasonic cleaner before being examined under a JEOL J.S.M. U3 scanning electron microscope operating in the secondary electron image mode at 25 kV. For elemental analysis of the fracture surface, an EDAX 505 energy-dispersive X-ray analyser attached to the electron microscope was employed. The area of observation was confined mainly to the central 10 mm of test piece width and up to about 15 mm behind the fatigue crack tip.

The 0.2% proof stress of the material was determined from tensile specimens machined from the fractured half of the compact tension specimen. The axis of the tensile specimen was perpendicular to the crack plane in the compact tension specimen. At least two tensile specimens were tested at each tempering temperature.

## 3. Results and discussion

### 3.1. Effect of tempering temperature

The effects of tempering temperature on the 0.2% proof stress and the plane strain fracture toughness, $K_{IC}$, of Comsteel En25 in the R–L or C–L crack plane orientation are shown graphically in Fig. 1. It can be seen that the proof stress, $\sigma_{ys}$, of the material decreased with increasing tempering temperature over the entire temperature range studied. Distinct yield plateaux were observed for

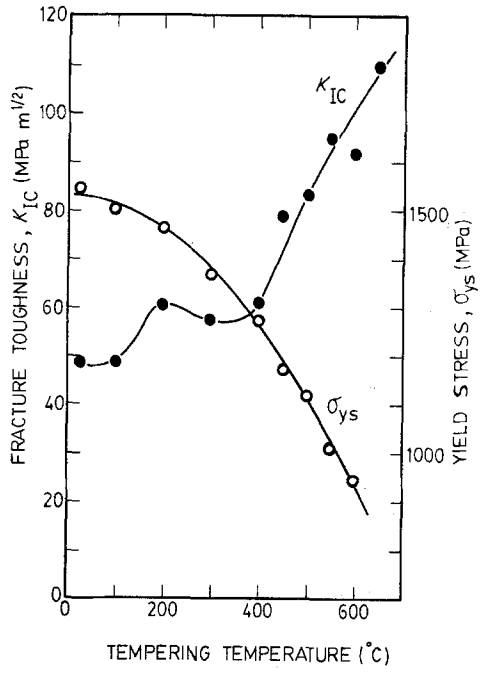


*Figure 1* Effect of tempering temperature on 0.2% proof stress and plane strain fracture toughness.

all specimens tempered at 300° C and above. The average plane strain fracture toughness of the material in the as-quenched condition was 48.5 MPa m$^{1/2}$. This remained approximately constant at 100° C but increased abruptly to 60.6 MPa m$^{1/2}$ at 200° C. Tempering at 300° C, however, produced a slight but distinct drop in the toughness value indicating the occurrence of tempered martensite embrittlement at approximately 350° C. At 400° C and above, the fracture toughness was found to increase steadily with increase in tempering temperature. The general trend of $K_{IC}$ variation with tempering temperature is similar to that often observed [6, 7]. A fine martensitic network with an average grain size of about 7 $\mu$m was observed for the steel at all tempering temperatures.

At low magnification, the overload fracture surface of the as-quenched specimen was rather flat and featureless, with a few elongated MnS inclusions (Fig. 2). The line of demarcation between fatigue crack and overload fracture was difficult to define, although generally the fracture mode at the tip of the crack was smooth intergranular with extensive secondary cracks, as can be observed in Fig. 3. (Note that the direction of crack propagation is from the bottom of the figure towards the top.) Immediately in front of

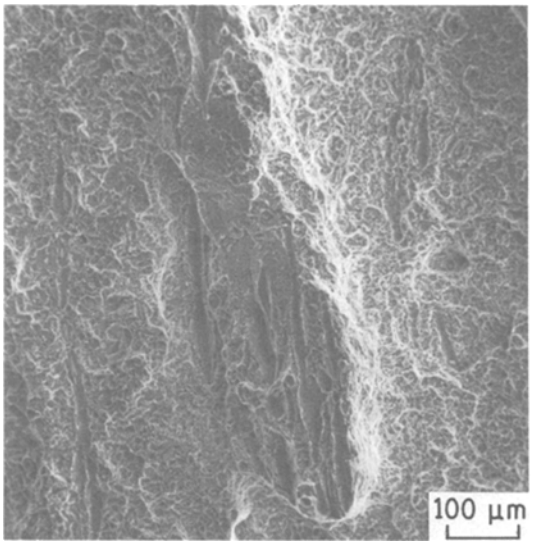


*Figure 2* As-quenched specimen: overall fracture surface of overload region. Direction of crack propagation from bottom to top.

the fatigue crack, the fracture was a mixture of dimples and cleavage facets. This was carried on to the main overload region, where the fracture mode contained approximately equal proportions of dimples and cleavage. Many of the dimples contained small impurity particles which were analysed to consist of MnS.

The fracture morphology of the 100° C tempered specimen was almost identical to that in the as-quenched state. This is reflected in the

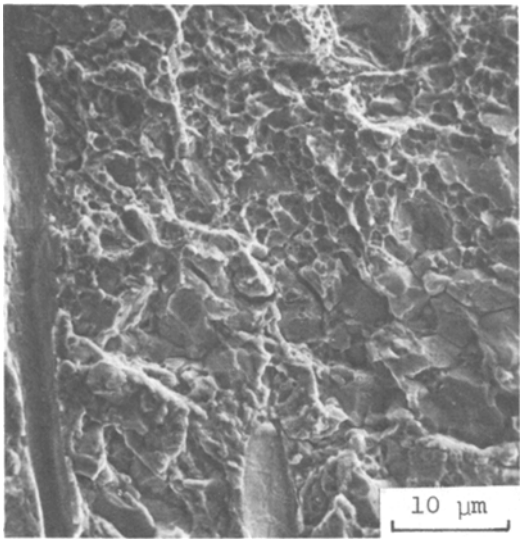


*Figure 3* As-quenched specimen: fracture morphology at crack tip.

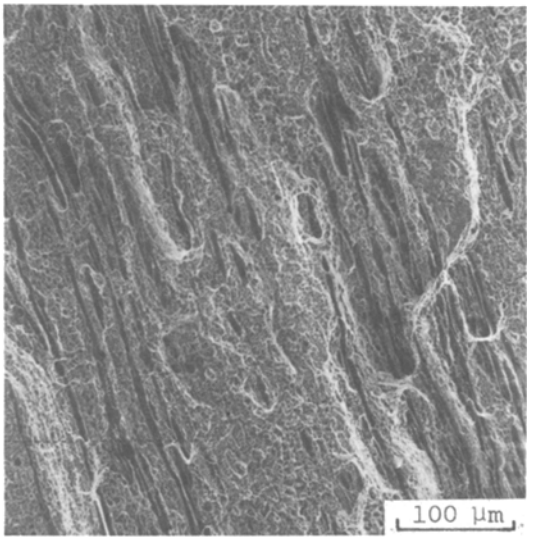


*Figure 4* 200° C temper: overall fracture surface at overload region.

approximately equal value of the fracture toughness (48.7 MPa $m^{1/2}$ in the 100° C temper as compared to 48.5 MPa $m^{1/2}$ in the as-quenched). However, tempering at 200° C produced a nearly 20% increase in fracture toughness over that in the as-quenched state. As shown in Fig. 4, the overload region in the 200° C tempered specimen showed a large number of stringers being exposed during the fracture, and the overall surface became more rugged. The higher fracture toughness value is the result of the increase in surface relief due to the formation of steep and abrupt shear facets between different layers or bands of MnS stringers. Stereofractographs show that the crack front appeared to change its direction by adopting a shearing mechanism to link up layers of MnS inclusions at different elevations. The shear planes were generally observed to be perpendicular to the plane of crack propagation. Consequently, the crack advanced in a stepwise manner resulting in a terrace-type fracture surface with "plateaux" or "steps" of lengths equal to those of the MnS stringers. A typical example of such a fracture path is shown in Fig. 5. A similar type of fracture has been observed in steels in the short-transverse orientation [8, 9] and also in aluminium alloys [10]. The crack tip of the 200° C tempered specimen could be clearly identified. The immediate crack tip contained mainly ductile dimple fracture, and even in the overload region the fracture morphology was observed to be ductile dimple fracture. Cleavage facets, which were

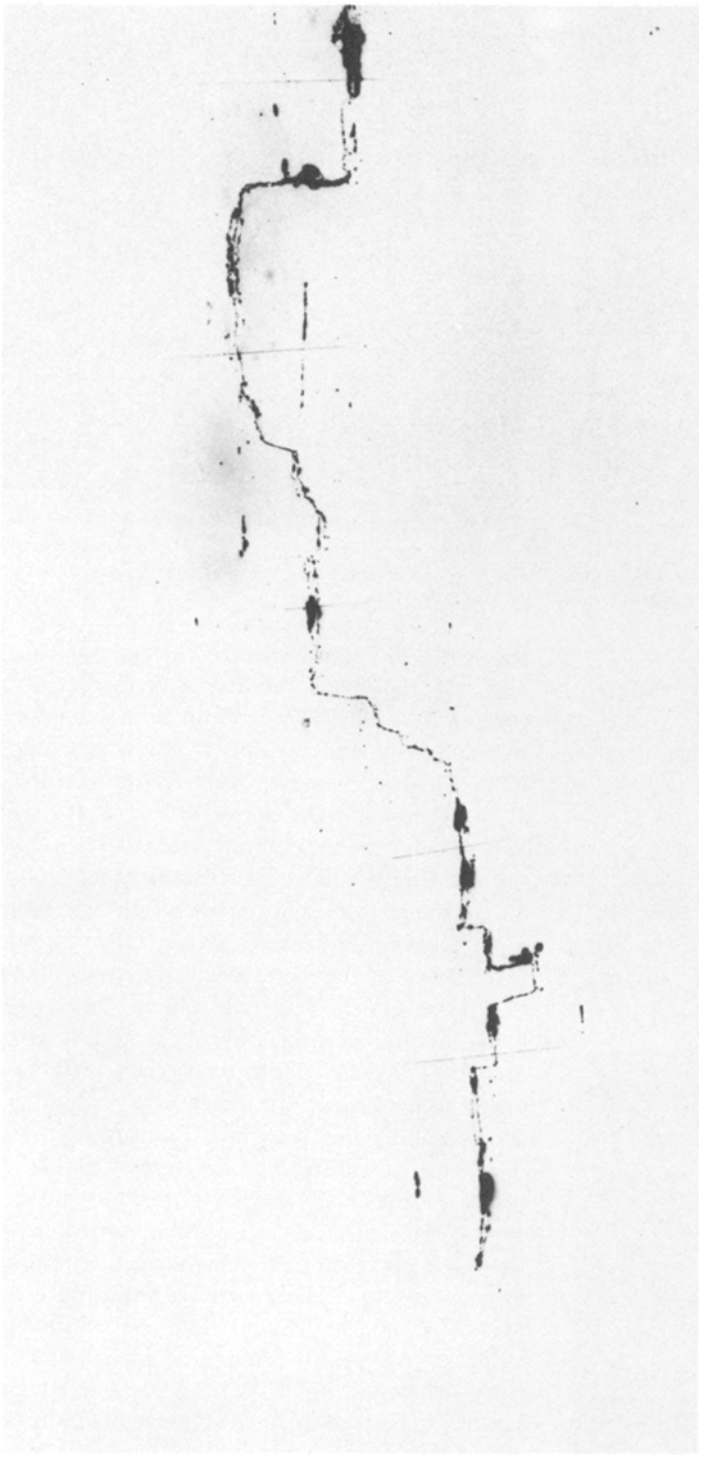

*Figure 5* Typical example of terrace-type fracture path.

commonly observed in the as-quenched and 100° C tempered specimens, were found to occur only in a few isolated areas.

As can be seen from Fig. 1, a noticeable drop in fracture toughness occurred as the tempering temperature was increased to 300° C. The decrease in toughness value is accompanied by significant changes in fracture morphology. Although the main fracture region at low magnification still appeared to be relatively similar to that at 200° C

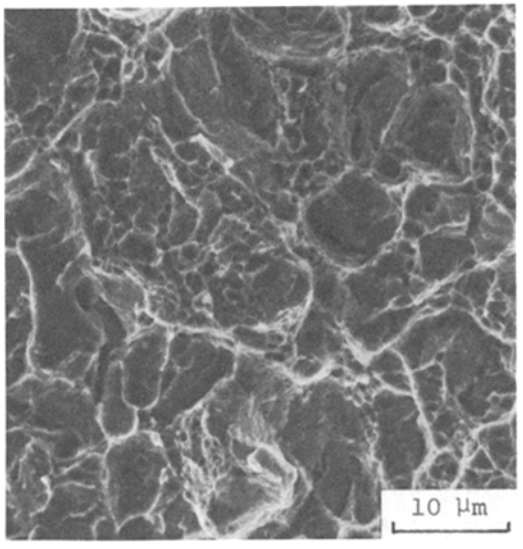


*Figure 6* 300° C temper: cleavage fracture at overload region.

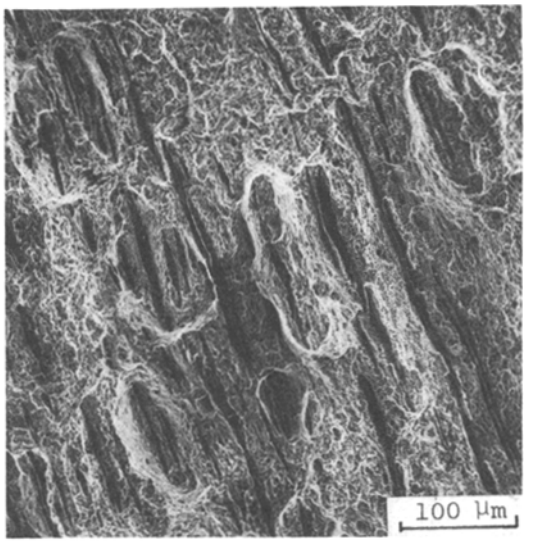


*Figure 7* 400° C temper: overall fracture surface at overload region.

tempering temperature, in that the surface was equally uneven and consisted of numerous stringers, the fracture mode at high magnification was one of extensive cleavage facets. At the crack tip, the morphology was a mixture of ductile dimples and cleavage, but as the crack propagated the latter fracture mode dominated the larger part of the feature, as can be observed in Fig. 6. The size of the cleavage facet was estimated to be about the size of the grain. At this tempering temperature, a significant increase in the precipitation of cementite occurred in the microstructure of the material. Clark [11], using the same material, found that the cementite precipitated within the martensite laths and along the lath boundaries. He suggested that the tempered martensite embrittlement is the result of the reduction in cohesive strength of the martensite–ferrite interface caused by impurities rejected when the cementite particle grows [12].

Tempering at 400° C produced a further increase in surface relief as shown in Fig. 7 (as compared to Fig. 6 for 300° C temper). The crack tip was characterized by dimples, while the main fracture morphology consisted of a large proportion of cleavage fracture (Fig. 8). Although the fracture toughness value at 400° C was approximately equal to that at 200° C, the predominant fracture mode for the 200° C temper was, however, ductile dimples. The difference is therefore the consequence of tempered martensite embrittlement in the 400° C tempered material. Because of the lower yield stress in the 400° C temper, the plastic zone size, which is proportional to $(K_{IC}/\sigma_{ys})^2$, is larger than in the 200° C temper. The large plastic zone produces a greater surface relief, since there is a higher probability of encountering a MnS inclusion at a greater distance from the crack plane as the crack propagates. The ductile dimples formed in the 400° C temper, however, appeared to be deeper and larger indicating that the material was more ductile than that tempered at 200° C.

Further reduction in yield stress was seen when

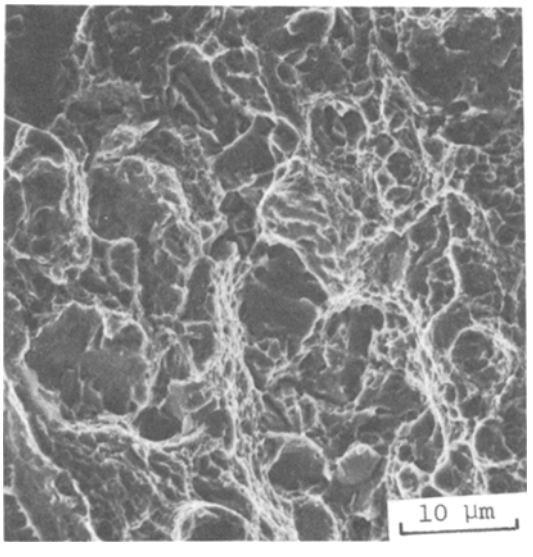


*Figure 8* 400° C temper: cleavage fracture at overload region.

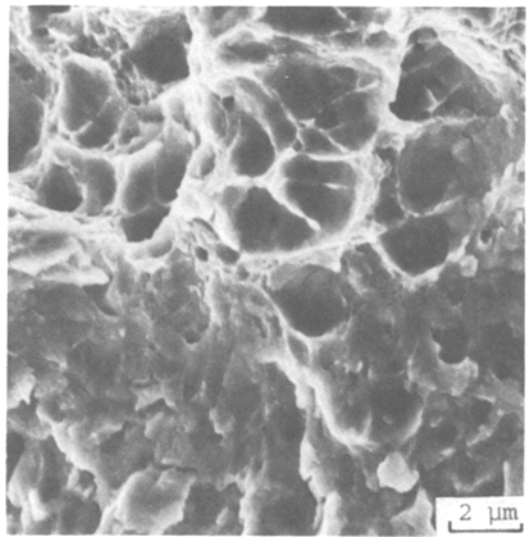


*Figure 9* 450° C temper: stretched zone at crack tip.

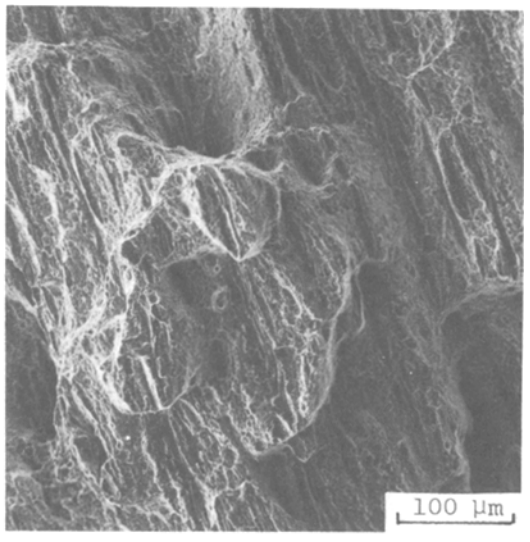


*Figure 10* 600° C temper: overall fracture surface of overload region.

the material was tempered at 450° C. Unlike the 400° C tempered specimens, here the fracture toughness was found to increase considerably. Cleavage fracture indicating a tempered martensite embrittlement region could no longer be found. The fracture morphology consisted of ductile dimples and abrupt shear facets that linked bands of MnS inclusions on different planes thus forming terrace-type fracture. Well-formed ductile dimples were found on flat areas between stringer troughs and at the immediate crack tip. Stereofractographs of the crack tip showed a well-formed stretched zone (Fig. 9). It has been observed [11] that at this tempering temperature the cementite in the material changes from needle-like to a shorter cylindrical precipitate, with some of the precipitates even spheroidizing. A discernible amount of through-thickness contraction occurred at the surfaces of the fractured specimens, further indicating an increase in ductility of the material.

The fracture surfaces of the material tempered at 500, 550 and 600° C were very similar to one another. The surface relief in the overload region increased steadily with tempering temperature, so that at high tempering temperatures the surfaces were extremely uneven and rugged, with a large amount of MnS stringers and stringer troughs being exposed. Fig. 10 shows a typical example of the fracture surface in the overload region at 600° C temper. The immediate crack tips were dominated by shear and ductile dimples as shown in Fig. 11. In the flat areas between stringers, ductile dimples were observed. The path of crack propagation was generally one of shear from inclusion bands to inclusion bands, resulting in terrace-type fracture (Fig. 10).

## 3.2. Effect of anisotropy

Fracture features of the 500° C tempered specimens in the R–L, L–R and R–C orientations are shown in Figs. 12, 13 and 14 respectively. In the R–L orientation, a terrace-type fracture was observed that resulted from shear facets linking bands of MnS stringers at different elevations.

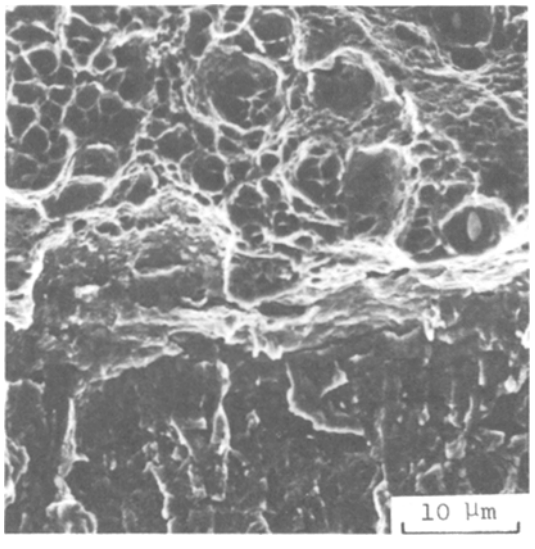


*Figure 11* 550° C temper: fracture morphology at crack tip.

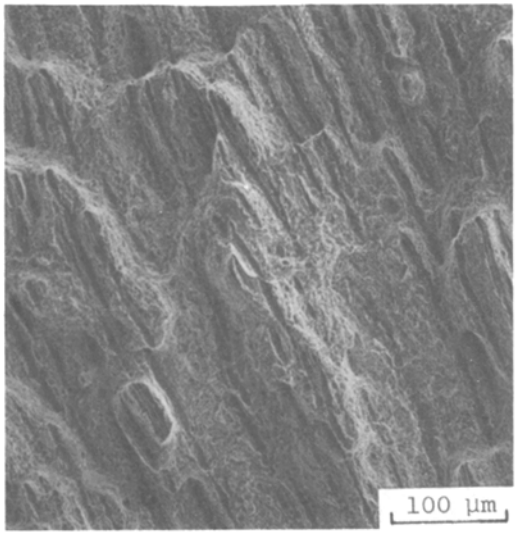


*Figure 12* 500° C temper (R–L orientation): overall fracture surface of overload region.

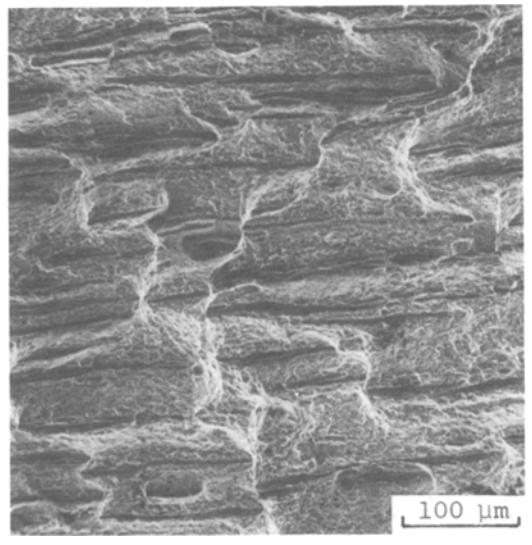


*Figure 14* 500° C temper (R–C orientation): overall fracture surface of overload region.

Very similar fracture features were seen in the R–C orientation, although very frequently the terrace-type fracture developed into a zigzag type topography similar to those previously observed in high-strength steels [13, 14]. This zigzag appearance was the consequence of shear fracture from inclusion to inclusion, with each trough or peak in the fracture surface ending at an MnS stringer which was parallel to the crack front. Well-formed dimples were found in areas between inclusions. Steep shear facets and dimples were the dominant features at the immediate crack tip. The high fracture toughness (83.7 and 87.4 MPa $m^{1/2}$ for R–L and R–C orientations respectively) and relatively low yield stress at this tempering temperature gave rise to high surface relief (Figs. 12 and 13).

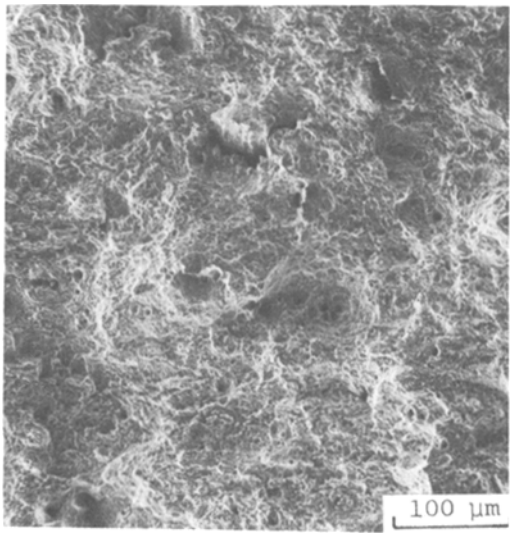


*Figure 13* 500° C temper (L–R orientation): overall fracture surface of overload region.

On the other hand, the fracture morphology in the L–R orientation as shown in Fig. 13 was in general flat and featureless, even though the fracture toughness was as high as 150.4 MPa $m^{1/2}$. No terrace or zigzag-type fracture was observed. At the immediate crack tip, the fracture was essentially ductile dimple rupture. Secondary cracks were however frequently seen at the demarcation between the fatigue and the overload regions. Numerous cavities formed around the MnS inclusions were commonly found in the fast-fracture region. This is illustrated in Fig. 15. The variation of fracture toughness value with crack plane orientation in Comsteel En25 is the result of the non-uniform distribution of non-metallic inclusions. Because of the hot rolling process, the major inclusions were found to be, for all tempering temperatures, Type II inclusions of MnS. These were aligned such that their long dimension was parallel to the rolling direction. In the L–R orientation, therefore, the crack must cut across the stringers with decohesion and fracturing of the stringers taking place in the process; but with the R–C and R–L orientations the crack encountered a much larger projected area of inclusions, and these were potential sources of

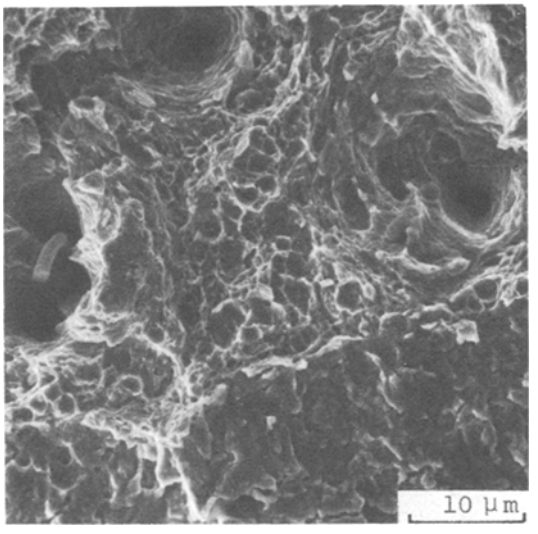


*Figure 15* 500° C temper (L–R orientation): fracture morphology at crack tip.

fracture initiation and propagation path due to delamination between inclusions and the surrounding matrix.

Crack propagation along the length of the inclusion required little energy since the bond between inclusion and matrix is generally weak. Moreover, crack propagation tends to take the direction of least resistance to matrix fracture [8]. Neal and Doig [15] observed that when the MnS inclusions were stressed across the minor axis as in the case of short-transverse or R–L orientation, cracking occurred along the inclusion matrix boundary; but when the inclusions were stressed along their major axis, the inclusions fractured before the matrix. It can be inferred that in the L–R orientation, fracture occurred mainly by the nucleation of voids at inclusion particles and hence required more energy for propagation. Fegredo [16] working with plain C–Mn steel showed that the maximum load required to fracture WOL-type (wedge open loading type) specimens in the L–T orientation was nearly twice that in the S–L orientation. Because of the vast difference in fracture load, most specimens were reported to have crack planes turned through 90° to progress along the longitudinal direction. A fracture toughness value in the L–R orientation of 1.8 times that in the R–L orientation for Comsteel En25 is therefore not unreasonable,

## 4. Conclusion

From the present study, it can be seen that the fracture toughness of Comsteel En25 is very much related to the surface topograph of the test specimen. The anisotropic effects are a direct consequence of the non-uniform distribution of inclusions and the anisotropy in their shape. The R–L or short transverse crack plane orientation suffers the most, as a result of the alignment of the elongated MnS inclusions in a direction parallel to the crack propagation.

## References


R. E. ZINKHAM, *Eng. Fract. Mech.* **1** (1968) 275.
2. J. G. KAUFMAN, R. L. MOORE and P. E. SCHILLING, *ibid.* **2** (1971) 197.
3. F. G. NELSON and J. G. KAUFMAN, ASTM STP 536 (American Society for Testing and Materials, Philadelphia, 1973) p. 350.
4. R. P. WEI, ASTM STP 381 (American Society for Testing and Materials, Philadelphia, 1965) p. 279.
5. A. S. TETELMAN and A. J. MCEVILY, in "Fracture – An Advanced Treatise," Vol. 6 (Academic Press, London, 1969) p. 137.
6. J. E. KING, R. F. SMITH and J. F. KNOTT, Proceedings of the 4th International Conference on Fracture, Waterloo, Canada, Vol. 2A, edited by D. M. R. Taplin (1977) p. 279.
7. K. H. SCHWALBE and W. BACKFISH, Proceedings of the 4th International Conference on Fracture, Waterloo, Canada, Vol. 2A, edited by D. M. R. Taplin (1977) p. 73.
8. T. J. BAKER, K. B. GOVE and J. A. CHARLES, *Metals Tech.* **3** (1976) 183.
9. R. H. SAILORS, ASTM STP 600 (American Society for Testing and Materials, Philadelphia, 1976) p. 172.
10. C. J. PEELE, R. N. WILSON and P. J. E. FORSYTH, *Metal Sci.* **6** (1972) 102.
11. N. E. CLARK, PhD thesis, University of Auckland, 1976.
12. J. R. RELLICK and C. J. MCMAHON, *Metall. Trans.* **5** (1974) 2439.
13. C. F. CHIPPERFIELD and J. F. KNOTT, *Metals Tech.* **2** (1975) 45.
14. C. D. BEACHEM and G. R. YODER, *Metall. Trans.* **4** (1973) 1145.
15. B. NEAL and A. DOIG, in "Practical Implications of Fracture Mechanisms," Inst. Metallurgists meeting, spring 1973, p. 145.
16. D. M. FEGREDO, *Canadian Metall. Quarterly* **14** (1975) 243.



*Received 30 April*
*and accepted 6 July 1984*